Supplementary Materials

Abnormal mTORC1 signaling leads to retinal pigment epithelium degeneration

Jiancheng Huang, Shun Gu, Meng Chen, Shu-jie Zhang, Zhichun Jiang, Xue Chen, Chao Jiang, Guohua Liu, Roxana A Radu, Xiantao Sun, Douglas Vollrath, Jianhai Du, Biao Yan, Chen Zhao

Supplementary Methods

Western blot

The lysates were separated on SDS-polyacrylamide gels, and then transferred to polyvinylidene fluoride membrane (PVDF) (Millipore, Bedford, MA, USA). The membrane was blocked with 5% skim milk for 1 hour at 37°C, incubated with the primary antibody at 4°C overnight (Supplementary Table 2), washed with 1×TBST, and incubated with the horseradish peroxidase (HRP)-conjugated secondary antibodies (1:10000, Sigma-Aldrich, St. Louis, MO, USA) for 1 hour at room temperature. The blots were visualized by the ECL-Western blotting system (Tanon, Shanghai, China). Protein expression was quantified using Image J software.

Paraffin histology

Eyecups for paraffin histology were prepared and fixed as described for cryosections, and then dehydrated in the graded ethanol series and embedded in paraffin wax. Serial sectioning of the eyecup was performed at 5-μm thickness using a microtome (Leica, Wetzlar, Germany). Sections were deparaffinized in xylene, rehydrated through graded ethanol series, stained with hematoxylinand eosin (H&E), and observed using a microscope (Olympus, Tokyo, Japan).

Transmission electron microscopy

For transmission electron microscopy, eyecups were dissected in fixative (2.5% glutaraldehyde in 0.1 mol/L phosphate buffer, pH=7.2) immediately after enucleation, post-fixed in 1% osmic acid, rinsed in PBS, and then stained with aqueous 3% uranyl acetate for 2 hours. After being dehydrated in ascending concentrations of acetone, samples were embedded in epoxy resin (EPON 812). Samples were ultra-thin sectioned (Leica ultracut) into a thickness of 60~70 nm and stained with uranyl acetate and lead citrate. The sections were observed using the transmission electron microscopy (Tecnai G2 Spirit BioTWIN, FEI, USA).

Fundus photography

Mice were anesthetized intraperitoneally with a mixture of ketamine (100 mg/kg) and xylazine (10 mg/kg). Pupillary dilation was induced by 1% cyclopentolate- HCl and 2.5% phenylephrine. Funduscopic examination was performed using a binocular indirect ophthalmoscope (Kowa, Genesis D, Japan). Fundus images were obtained under appropriate illumination intensity.

Electroretinography (ERG)

ERG was recorded with an Espion system (Espion, Diagnosys, USA) according to the recommendations of the International Society for Clinical Electrophysiology of Vision. After dark adaption for 8 hours, ERG was performed under the dim red light. The pupils were dilated by 1% cyclopentolate-HCl and 2.5% phenylephrine. Waves were recorded in response to flashes at 0.01, 3.0, and 10.0 $cd \times s/m^2$.

Spectral-domain optical coherence tomography (SD-OCT)

RPE-TSC1$^{-/-}$ mice and littermate controls were anesthetized and their pupils dilated as previously described. Optical coherence tomography was performed with a spectral domain optical coherence tomography system (SD-OCT; OptoProbe, Burnaby, Canada). Lateral images (from nasal to temporal) crossing through the optic nerve were collected. Photoshop software (Adobe) was used to measure the thickness of retinal layers. Thickness measurements were done in a double-blind manner.

Supplementary Table

Table S1: Primers used in this study

Name	Forward (5'-3')	Reverse (5'-3')
Cre	ATTTGCCTGCATTACCGGTC	ATCAACGTTTTCTTTTCGG
TSC1 loxP	GTCACGACCGTAGGAGAAGC	GAATCAACCCCACAGAGCAT
TSC1 KO	TGGAGGTAACGTTGCTTCAG	TGAGGGTACTACAGCGACATC
rd1	CATCCCACCTGAGCTCACAGAAAG	ACTGGGCAAAGTGAACAGC
rd8	GGTGACCAATCTGTTGACAATCC	GCCCCATTTGCACACTGATGAC

Table S2: Antibodies used in this study

Antigen	Host	Immunostaining	Immunoblot	Supplier
Primary antibodies				
Cre	mouse	1:200	no	Millipore
TSC1	rabbit	1:200	no	Abcam
S6	rabbit	no	1:1000	Cell Signaling
p-S6(Ser235/236)	rabbit	1:200	1:1000	Cell Signaling
p70S6k	rabbit	no	1:1000	Cell Signaling
p-p70s6k(Thr389)	rabbit	no	1:1000	Cell Signaling
RPE65	mouse	1:400	no	Millipore
MERTK	rabbit	no	1:1000	Abcam
LRAT	rabbit	no	1:1000	Abcam
Kertain18	mouse	no	1:1000	Abcam
β-catenin	rabbit	1:200	no	Cell Signaling
β-actin	mouse	no	1:1000	Cell Signaling
p-Akt(Ser473)	rabbit	no	1:1000	Cell Signaling

Akt	rabbit	no	1:1000	Cell Signaling
p21	rabbit	no	1:1000	Cell Signaling
p27	rabbit	no	1:1000	Cell Signaling
Secondary antibodies				
DAPI		1:2000	no	Vector
Goat anti mouse 594		1:400	no	Pierce
Dunkey anti mouse 488		1:400	no	Life technology
Goat anti rabbit 488		1:400	no	Life technology
Dunkey anti rabbit 594		1:400	no	Life technology
Goat anti mouse IgG (H+L) HRP			no	1:10000 Invitrogen
Goat anti rabbit IgG (H+L) HRP			no	1:10000 Invitrogen
Lectin				
Phalloidin 594		1:100	no	Life technology

57

58 **Table S3: Liquid Chromatography/MS-MS metabolites table**

Compound	Human Metabolome Database（HMDB）	PubChem	Q1
NAD	HMDB00902	5893	664
4-Hydroxyproline	HMDB00725	5810	132.1
L-Proline	HMDB00162	145742	116.1
NADP	HMDB00217	5886	744
NADPH	HMDB00221	22833512	746
L-Arginine	HMDB00517	6322	175.1
Nicotinamide ribotide	HMDB00229	14180	335
nicotinamide riboside	HMDB00855	439924	255.1
L-Glutamine	HMDB00641	5961	147.1
Adenosine triphosphate	HMDB00538	5957	507.9
Niacinamide	HMDB01406	936	123
Trigonelline	HMDB00875	5570	138
1-Methylnicotinamide	HMDB00699	457	137
3-Hydroxybutyric acid	HMDB00357	441	105.1
	N/A	76972985	126
Uridine diphosphate glucose	HMDB00286	53477679	611
Choline	HMDB00097	305	104.1
	HMDB00201	7045767	204.1
FAD	HMDB01248	643975	786.1
Riboflavin	HMDB00244	493570	377.1

Carnosine	HMDB00033	439224	227.1
Coenzyme A	HMDB01423	6816	768.1
AICAR	HMDB01517	65110	259.1
Malonyl-CoA	HMDB01175	10663	854.1
	HMDB01206	444493	810.1
	HMDB02322	273	103
Tyramine	HMDB00306	5610	138
Adenosine	HMDB00050	60961	268.1
Spermine	HMDB01256	1103	203.1
Trimethylamine N-oxide	HMDB00925	1145	76
L-Cysteine	HMDB00574	5862	122.1
	HMDB03331	27476	282.1
Creatine	HMDB00064	586	132.1
Cytidine	HMDB00089	6175	244
Histamine	HMDB00870	774	112
Glycerol	HMDB00131	753	93
Guanosine	HMDB00133	6802	284.1
L-Cystathionine	HMDB00099	439258	223.1
Betaine	HMDB00043	247	118.1
Guanosine diphosphate	HMDB01201	8977	444
L-Homoserine	HMDB00719	12647	120.1
L-Tryptophan	HMDB00929	6305	205
L-Aspartic acid	HMDB00191	5960	134.1
Guanosine monophosphate	HMDB01397	6804	364.1
Sarcosine	HMDB00271	1088	90
dUMP	HMDB01409	65063	307
	HMDB01491	1051	246
	HMDB03911	64956	104.1
Thiamine	HMDB00235	1130	265
Cyclic AMP	HMDB00058	6076	328
Cyclic GMP	HMDB01314	24316	344
Glutathione	HMDB00125	124886	306
	HMDB03337	65359	611
Adenosine monophosphate	HMDB00045	6083	346
NADH	HMDB01487	928	664
Creatinine	HMDB00562	588	112
Ascorbic acid	HMDB00044	54670067	175
Quinolinic acid	HMDB00232	1066	166
L-Kynurenine	HMDB00684	161166	207.1
Nicotinic acid	HMDB01488	938	122
Oxalacetic acid	HMDB00223	970	131
D-Glucose	HMDB00122	5793	179
Guanosine triphosphate	HMDB01273	6830	521.9
Hypoxanthine	HMDB00157	790	135

Aminoadipic acid	HMDB00510	469	160.1
Citrulline	HMDB00904	9750	174.1
Azelaic acid	HMDB00784	2266	187
Adenine	HMDB00034	190	134
Uracil	HMDB00300	1174	111
Xanthine	HMDB00292	1188	151
Maleic acid	HMDB00176	444266	115
Hippuric acid	HMDB00714	464	178
	HMDB00532	10972	116
	HMDB00072	643757	173
	HMDB00210	167945	218.1
Dihydroxyacetone phosphate	HMDB01473	668	169
D-glyceraldehyde 3-phosphate	HMDB01112	729	169
4-Hydroxyphenylpyruvic acid	HMDB00707	979	179.1
Xanthosine	HMDB00299	64959	283.1
Citraconic acid	HMDB00634	643798	129
Glutaric acid	HMDB00661	743	131
Guanosine	HMDB00133	6802	282.1
L-Cystathionine	HMDB00099	439258	221.1
Salicylic acid	HMDB01895	338	137
Guanosine diphosphate	HMDB01201	8977	442
Pyruvic acid	HMDB00243	1060	87
Inosine	HMDB00195	6021	267
ADP	HMDB01341	6022	426
Guanosine monophosphate	HMDB01397	6804	362.1
Xanthurenic acid	HMDB00881	5699	204
Heptadecanoic acid	HMDB02259	10465	269.1
Glyceric acid	HMDB00139	439194	105
Methylmalonic acid	HMDB00202	487	117
Glucose 6-phosphate	HMDB01401	5958	259
Inosinic acid	HMDB00175	8582	347
Uridine 5'-diphosphate	HMDB00295	8629	403
	N/A	10935	97

Supplementary Figure legends

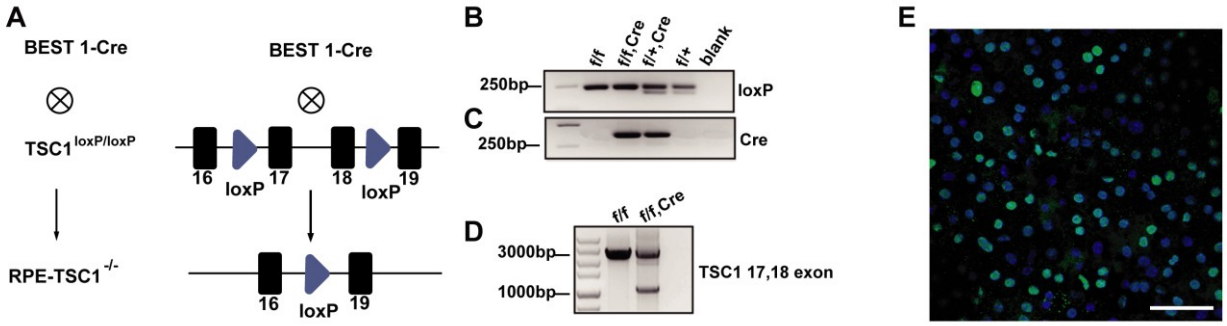

Figure S1: Conditional knockout of TSC1 in RPE

(A) Strategy for generating mice with RPE-specific deletion of TSC1. (B and C): Genotyping of mice by PCR analysis of genomic DNA. The bands corresponding to the wild-type (193 bp, WT) and loxP (230 bp, fl) TSC1 alleles were indicated. Cre genotype (350 bp) was also confirmed. (D) Genomic PCR analysis of deletion of TSC1 exon 17 and 18 in RPE-choroid complex from control (2727 bp) and RPE-TSC1$^{-/-}$ mice (1473 bp). (E) Approximately 70% of total RPE cells expressed Cre (green) in RPE-TSC1$^{-/-}$ mice (Scale bar: 20 μm).

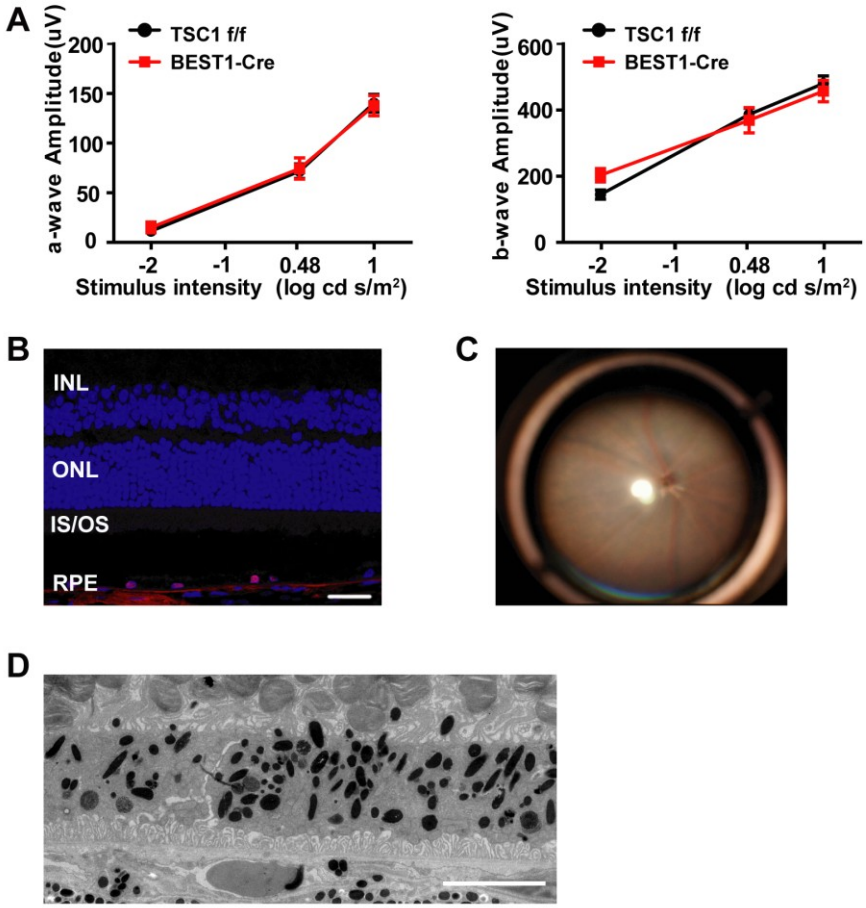

Figure S2: Absence of Cre toxicity in mice

(A) Electroretinography showed no difference in scotopic a-wave and b-wave between 5-month-old $TSC1^{f/f}$ mice (n=5) and $TSC1^{WT/WT}$; +/Tg (BEST1-cre) mice. (n=5); Mean ± standard deviation. (B) Immunofluorescence for Cre (red) was detected in 6-month-old $TSC1^{WT/WT}$; +/Tg (BEST1-Cre) mice (Scale bar: 25 µm). (C) Fundus image of 6-month-old $TSC1^{WT/WT}$; +/Tg (BEST1-Cre) was shown. (D) $TSC1^{WT/WT}$; +/Tg (BEST1-cre) mice had normal RPE ultrastructure at 6 month (Scale bar: 5 µm).

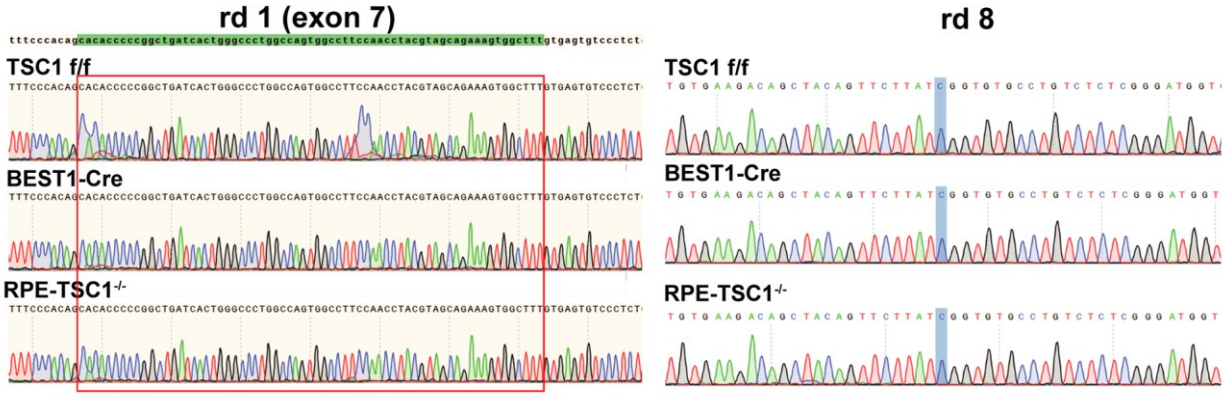

Figure S3: Sequencing chromatograms of rd1 and rd8

Sequencing chromatograms of the rd1 and rd8 of genomic regions from $TSC1^{f/f}$, BEST1-Cre, and RPE-$TSC1^{-/-}$ mice, respectively (Top). No mutations were found.